Biochar X https://doi.org/10.48130/bchax-0026-0015

Original Research Open Access

An oxygen-nanobubble-loaded biochar for cadmium stabilization in contaminated paddy soil

Qingnan Chu[1#], Detian Li[1,2#], Shuhan Xu[1], Dongrong Pan[1], Haoyu Cao[1], Hui Gao[1], Chengming Zhang[1,3], Shanliang Liu[4], Bin Liu[5], Wenjia Chen[5], Qiuyue Wang[6], Jinghua Wu[6], Ping He[7*] and Zhimin Sha[1*]

Received: 23 April 2026

Revised: 2 May 2026

Accepted: 27 May 2026

Published online: 9 June 2026

Abstract

In flooded Cd-contaminated paddy soils, conventional biochar amendments often function mainly as passive sorbents, and their immobilization efficiency can be constrained by rapid oxygen depletion and the reductive dissolution of Fe/Mn phases. However, whether oxygen-loaded biochar can overcome this limitation and outperform Fe-loaded biochar, and how redox regulation, Cd speciation, and rhizosphere microbial functions jointly control plant Cd uptake, remain insufficiently understood. Here, oxygen-nanobubble-loaded biochar (ONBC) was developed as an active micro-oxygenation amendment for Cd stabilization in contaminated paddy soil. In a rice pot experiment, ONBC was compared with pristine biochar (BC), Fe-loaded biochar (FeBC), and an unamended control to evaluate its effects on rhizosphere redox conditions, Cd speciation, plant Cd accumulation, and microbial functions. ONBC maintained dissolved oxygen at 3–4 mg L^{-1} and positive rhizosphere redox potentials of approximately 100–300 mV during flooding, whereas the other treatments rapidly approached near-anoxic conditions. Relative to the control, ONBC decreased exchangeable Cd by 2.9-fold, reduced carbonate-bound Cd by 96.6%, and lowered Cd concentrations in roots and shoots by 2.7- and 1.9-fold, respectively. Metagenomic analyses showed that ONBC increased bacterial diversity, enriched Fe/Mn-oxidizing taxa, enhanced microbial Cd efflux and detoxification functions, and stimulated C, N, and P turnover. Structural equation modeling further indicated that ONBC suppressed plant Cd mainly through redox- and microbiome-driven shifts in soil Cd speciation. These findings demonstrate that oxygen loading transforms biochar from a passive sorbent into an active rhizosphere-regulating platform, providing a novel strategy for stabilizing Cd in flooded paddy systems.

Keywords: Biochar, Cadmium, Carbonaceous materials, Metagenomics, Paddy soil, Rhizosphere redox

Highlights

- ONBC maintained oxic rhizosphere conditions in flooded Cd-contaminated soil.
- ONBC shifted Cd from labile pools to Fe/Mn oxide-bound and residual forms.
- ONBC enriched Fe/Mn-oxidizing taxa and microbial Cd detoxification genes.

# Authors contributed equally: Qingnan Chu and Detian Li

* Correspondence: Ping He (heping02@caas.cn); Zhimin Sha (zhiminsha@sjtu.edu.cn)

Full list of author information is available at the end of the article.

https://doi.org/10.48130/bchax-0026-0015

Graphical abstract

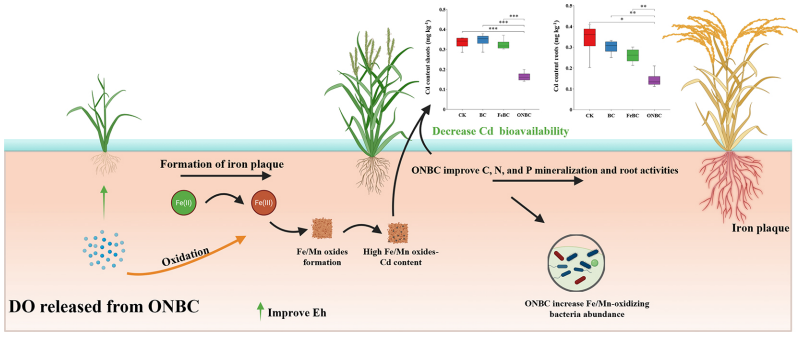

Introduction

Cadmium (Cd) is a non-essential and highly toxic trace metal whose persistence in agricultural soil poses simultaneous risks to ecosystem function, crop quality, and human health[1,2]. Rice (*Oryza sativa* L.) is especially vulnerable because flooded cultivation alters redox conditions in ways that can increase Cd mobility and favor plant uptake[3–5]. The resulting transfer of Cd into edible biomass has become an important environmental and food-safety issue in many paddy-growing regions[1,6]. Surveys have estimated that approximately 1.3×10^5 ha of farmland is affected by Cd pollution, producing nearly 5.0×10^4 tons of Cd-contaminated rice each year[7]. Therefore, effective strategies to reduce Cd uptake by rice are urgently needed.

The behavior of Cd in flooded soil is strongly controlled by redox-sensitive interfaces[7,8]. Among the most important are Fe/Mn (hydr)oxides in the bulk soil and iron plaque (IP) on rice roots[9,10]. When oxygen is available, Fe(II) and Mn(II) can be oxidized to highly reactive mineral phases that adsorb or co-precipitate Cd. Under reducing conditions, these phases can dissolve or lose retention capacity, thereby increasing labile Cd pools. The challenge is therefore not only to add sorption sites, but also to maintain a rhizosphere redox regime that favors persistent immobilization.

Biochar has been widely applied in soil science, plant nutrient uptake, and ecosystem remediation[11–13] because it can improve soil physicochemical properties, enhance nutrient retention and availability, regulate microbial activity, and reduce the mobility or toxicity of environmental pollutants. Also, biochar is an attractive carbonaceous amendment for Cd-amended soils because its porosity, surface functional groups, alkalinity, and cation-exchange properties can lower metal mobility[12,13]. However, pristine biochar often behaves mainly as a passive sorbent. In flooded paddy soils, its performance can be constrained by rapid oxygen depletion and reductive dissolution of Fe/Mn phases[11,14]. For this reason, modified biochars that can regulate the rhizosphere environment, rather than simply add surface area, may provide a more durable route to immobilization[15,16].

Oxygen nanobubbles (ONBs) offer one such opportunity[11,14]. Their large gas-liquid interfacial area and long residence time allow oxygen to be retained and released more gradually than with conventional aeration[17]. When loaded into a carbon matrix, nanobubbles may transform biochar into an active micro-oxygenation material capable of maintaining higher dissolved oxygen, sustaining positive redox potential, promoting Fe/Mn oxidation, and reshaping microbial metabolism at the soil-root interface[11,14,18]. This concept is especially relevant in flooded systems, where metal fate emerges from coupled geochemical and biological feedbacks.

A second unresolved issue is whether oxygen loading provides a clearer functional advantage than Fe-loading alone. Fe-loaded biochar can increase Fe supply and stimulate IP formation, but without sustained oxygenation, its effects may be transient or context-dependent. Moreover, the relative contributions of bulk-soil immobilization, root-surface IP, and microbiome restructuring to plant Cd reduction remain insufficiently resolved in flooded paddy systems.

Here, ONBC and FeBC were prepared from the same parent biochar and tested in Cd-contaminated paddy soil planted with rice. We hypothesized that ONBC would outperform BC and FeBC because oxygen loading would: (i) sustain a more oxidizing rhizosphere during flooding; (ii) shift Cd from labile to stable fractions through coupled Fe/Mn cycling; and (iii) enrich microbial functions that reinforce Cd detoxification and nutrient turnover. By integrating rhizosphere redox monitoring, sequential Cd fractionation, plant analysis, metagenomics, and structural equation modeling, we aimed to clarify how an engineered oxygen-loaded carbonaceous material stabilizes Cd in flooded soil.

Materials and methods

Biochar preparation and characterization

Corn-straw-derived biochar was obtained from Henan Lize Environmental Protection Technology Co., Ltd. According to a previous study, the feedstock was pulverized, passed through a 1 cm sieve, pyrolyzed at 500 °C for 5 h in a muffle furnace under oxygen-limited conditions, cooled under N_2, and sieved to < 2 mm particle size. For Fe-loaded biochar (FeBC), 100 g of biochar was soaked in $FeCl_3$ solution (Fe^{3+} : C = 0.56:1, w/w) under ultrasonic agitation for 2 h to promote Fe impregnation. The mixture was then oven-dried at 105 °C for 12 h and pyrolyzed again at 500 °C for 2 h to stabilize the Fe loading. The final FeBC was sieved to < 2 mm and stored in airtight containers.

ONBC was prepared according to a previous study[18]. Briefly, 100 g of biochar was vacuum-treated at −0.1 MPa for 12 h and then exposed to high-purity oxygen (99.99%) at 0.2 MPa for 4 h in a pressure vessel. A cycle of vacuum extraction (2 h) followed by oxygen loading (6 h) was repeated once. The resulting ONBC was used immediately or stored under pressurized oxygen (0.15 MPa) until use. The oxygen-loading capacity of ONBC was quantified by sodium sulfite adsorption and an oxidation method. The releasable oxygen-loading amount was calculated as:

$$\text{Oxygen loading amount} = (DO_{ONBC} - DO_{BC}) \times V/m$$

where, DO_{ONBC} and DO_{BC} are the final dissolved oxygen (DO) concentrations in the ONBC and BC suspensions, respectively, V is the solution volume, and m is the dry mass of biochar. The ONBC

treatment showed a substantially higher oxygen-release capacity than BC, confirming successful oxygen loading. The calculated oxygen-loading amount was 15.6 mg O_2 g^{-1} biochar. Preparing FeBC and ONBC from the same parent biochar ensured identical feedstock and primary pyrolysis history. Basic physicochemical properties of BC, FeBC, and ONBC are listed in Supplementary Table S1.

Pot experiment and sampling

Paddy soil was collected from the top 0–20 cm of a Cd-contaminated agricultural field in Kunshan, Jiangsu Province, China (120°59′8.736″ E, 31°23′27.096″ N). The total Cd concentration was 1.17 mg kg $^{-1}$, exceeding the Chinese risk screening value of 0.6 mg Cd kg^{-1} for soils with pH ≤ 7.5 (GB 15618 -2018). Additional soil properties were as follows: pH (1:5, w/v) 6.17 ± 0.21, organic matter 50.05 ± 0.47 g kg^{-1}, total nitrogen 2.23 ± 0.15 g kg^{-1}, total phosphorus 0.46 ± 0.04 g kg^{-1}, total potassium 10.32 ± 0.14 g kg^{-1}, available nitrogen 148.22 ± 25.04 mg kg^{-1}, phosphorus 22.23 ± 4.98 mg kg^{-1}, and potassium 161.53 ± 21.63 mg kg^{-1}, respectively.

A pot experiment was conducted in a greenhouse at Shanghai Jiao Tong University (25–30 °C, 60%–70% relative humidity, and a 14-h photoperiod supplemented with LED lighting). Each pot contained 4 kg of air-dried Cd-contaminated soil mixed thoroughly with basal fertilizer. Rice (*Oryza sativa* L. cv. Qingjiao 307) seedlings were raised for 4 weeks before transplanting. Basal fertilizers were applied at 0.26 g urea, 1.17 g superphosphate, and 0.52 g potassium chloride per pot, followed by 0.26 g urea at tillering stage and 0.35 g urea at panicle initiation. These rates were equivalent to 240 kg N ha^{-1}, 120 kg P_2O_5 ha^{-1}, and 90 kg KCl ha^{-1}. Flooded conditions were maintained with a 4–6 cm water layer throughout cultivation. Treatments included: CK (no amendment), pristine biochar (BC at 1% w/w), iron-loaded biochar (FeBC at 1% w/w), and oxygen-nanobubble-loaded biochar (ONBC at 1% w/w), with four replicates per treatment in a completely randomized design.

Rhizosphere redox monitoring

During rice growth, soil redox potential (Eh), soil pH, and DO of overlying water were measured at 0, 10, 20, 30, 40, 50, 60, 70, 80, and 90 d after transplanting. Rhizosphere Eh was measured with a calibrated platinum electrode coupled with a reference electrode inserted 5–10 cm below the soil surface. Soil pH was measured using a Leici PHSJ-4F pH meter (Shanghai INESA Scientific Instrument Co., Ltd, Shanghai, China). The pH meter was calibrated with standard buffer solutions at pH 4.00, 7.00, and 10.00 before measurement. DO was recorded using a calibrated dissolved oxygen probe. The DO probe was calibrated with air-saturated water before measurement. All electrodes were rinsed with deionized water between samples and recalibrated before each measurement. Four biological replicates were measured for each treatment.

Plant analyses

At harvest, rice plants were gently removed from soil, washed, and separated into roots, shoots, and grains. Plant height, fresh weight, root length, root diameter, and root volume were recorded. Root porosity was determined by the pycnometer method, and root oxidative activity was quantified by the triphenyl tetrazolium chloride (TTC) reduction assay. Root antioxidant enzyme activities were determined following previous studies[18]. Briefly, superoxide dismutase (SOD) activity was determined by monitoring inhibition of nitroblue tetrazolium photoreduction, expressed as units per mg protein. Catalase (CAT) activity was assayed by monitoring H_2O_2 decomposition at 240 nm using a UV1700PC micro-spectrophotometer (Macylan Instruments Inc., Shanghai, China). Enzyme extracts were prepared from fresh root tissues by homogenization in phosphate buffer, followed by centrifugation at 12,000 rpm for 10 min at 4 °C, and the resulting supernatants were used for assays.

Root IP quantification and Cd analyses

IP on rice roots was extracted using dithionite-citrate-bicarbonate (DCB) solution. After fresh weight was recorded, roots were gently rinsed to remove loosely attached soil and immersed in DCB solution with gentle shaking for 30 min. Fe in the extracts was determined colorimetrically with o-phenanthroline at 510 nm using a UV1700PC micro-spectrophotometer. Cd in the extracted plaque was measured by inductively coupled plasma mass spectrometry (ICP-MS; Agilent 7900, Agilent Technologies, Santa Clara, CA, USA).

Soil Cd fractionation was determined by a modified Tessier sequential extraction method. Cd was partitioned into exchangeable (EXC), carbonate-bound (CARB), Fe/Mn oxide-bound (HOX), organic matter-bound (OM), and residual fractions (RES). Each extract was analyzed for Cd by ICP-MS after appropriate acid digestion. Additional details are provided in Supplementary Table S2.

Rice tissues, including roots and shoots, and bulk soil samples were oven-dried at 105 °C, ground, and digested with HNO_3–$HClO_4$. Total Cd concentrations were measured using ICP-MS with certified reference materials used for quality assurance. Multi-element standard solutions were used to establish calibration curves, and the correlation coefficients were required to be higher than 0.999. Method blanks, reagent blanks, duplicate samples, and certified reference materials for soil and plant tissues were included for quality assurance. The method detection limit for Cd was 0.001 mg kg^{-1} for solid samples. The recoveries of Cd in certified reference materials ranged from 90% to 110%, and the relative standard deviation of duplicate measurements was below 5%.

Metagenomic sequencing and annotation

Rhizosphere soil (approximately 0.5 g fresh weight per replicate) was collected at harvest. Total DNA was extracted using a silica-matrix soil DNA kit according to the manufacturer's instructions with bead-beating lysis. DNA integrity was verified by 1% agarose gel electrophoresis, and DNA concentration was determined using a Qubit 4.0 fluorometer (Thermo Fisher Scientific, Waltham, MA, USA). Samples were then subjected to metagenomic sequencing on an Illumina NovaSeq 6000 platform (Illumina Inc., San Diego, CA, USA) with paired-end 150 bp sequencing. Raw reads were filtered to remove adaptor sequences, low-quality reads, and reads shorter than 50 bp. Clean reads were retained only when the Q30 value was higher than 85%. Rarefaction curves were used to confirm that the sequencing depth was sufficient for downstream taxonomic and functional analyses.

Quality-filtered metagenomic reads were used for taxonomic annotation and abundance profiling. Alpha diversity (Chao1 richness and Shannon index) was calculated from the annotated bacterial community profiles. Genera with reported Fe/Mn-oxidizing capacity were matched to the genus abundance table, and their relative abundances were summarized for each treatment. Functional gene abundances associated with carbon (C), nitrogen (N), and phosphorus (P) mineralization and Fe-sulfur (S)-Mn redox cycling were obtained directly from the metagenomic data as KEGG Ortholog (KO) abundances. Target gene sets were then curated for analyses of Cd resistance and detoxification, nutrient turnover, redox cycling, and KEGG pathway enrichment.

Statistical analysis

Data were screened for normality and homoscedasticity before parametric analysis. Treatment effects on soil and plant variables,

enzyme activities, and selected taxa and gene groups were evaluated by one-way ANOVA followed by Duncan's multiple range test. Differences were considered statistically significant at $p < 0.05$. In figures, significance levels are indicated as follows: * $p < 0.05$; ** $p < 0.01$; and *** $p < 0.001$. A structural equation model (SEM) was constructed in SPSS-AMOS (IBM) to evaluate the effects of ONBC on plant Cd accumulation and growth performance. All four treatments were included in the SEM as categorical variables.

Genus-level bacterial data were further analyzed by orthogonal partial least squares discriminant analysis (OPLS-DA) in Simca-P (MKS Umetrics, Malmo, Sweden), following a previous study. Variable importance in projection (VIP) scores was calculated to rank genera contributing to separation among treatments, and score, VIP, and S-plots were used for visualization.

For heatmap visualization, each functional gene abundance value (counts per million, CPM) was standardized across samples by z-score normalization using $Z = (X - \mu)/\sigma$, where X represents the gene abundance in a given sample, μ is the mean abundance, and σ is the standard deviation of that gene across all samples. This row-wise normalization (mean = 0, SD = 1) emphasizes relative differences among treatments and was used for downstream visualization of functional gene profiles.

Results

ONBC changes the functional behavior of biochar under flooding

The most pronounced difference among treatments was their capacity to regulate the flooded rhizosphere environment. At the start of the experiment, DO was similar among treatments, ranging from 0.43 to 0.45 mg L^{-1}. After flooding, DO in the ONBC treatment increased rapidly to 4.23 mg L^{-1} at day 10 and remained within 2.20–3.59 mg L^{-1} from day 20 to day 90. By contrast, DO in CK and BC remained much lower, with final values of 0.53 and 0.64 mg L^{-1} at day 90, respectively. FeBC showed an intermediate response, with DO increasing to 1.78 mg L^{-1} at day 90. Over the 10–90 d monitoring period, mean DO followed the order ONBC > FeBC > BC ≈ CK, with average values of 2.99, 1.55, 1.25, and 1.19 mg L^{-1}, respectively. At day 90, DO in ONBC was approximately 4.9-, 4.1-, and 1.5-fold higher than that in CK, BC, and FeBC, respectively (Fig. 1a).

A similar trend was observed for rhizosphere redox potential. Although all treatments had the same initial Eh value of 439 mV, Eh declined rapidly during flooding in CK, BC, and FeBC. At day 90, Eh decreased to −10.6 mV in CK, 101.1 mV in BC, and 35.9 mV in FeBC, whereas ONBC maintained a positive Eh of 125.2 mV. Across the 10–90 d period, ONBC maintained the highest mean Eh value of 242.3 mV, compared with 140.9 mV in BC, 116.7 mV in FeBC, and 110.8 mV in CK. These results indicate that ONBC substantially delayed the development of reducing conditions in flooded soil and maintained a more oxidizing rhizosphere than the other treatments (Fig. 1b).

Soil pH also varied among treatments during rice growth. All treatments shifted from near-neutral pH at the beginning of the experiment to weakly alkaline conditions during the middle-growth stage. CK and BC reached maximum pH values of 8.92 and 9.38, respectively, whereas FeBC and ONBC reached maximum values of 8.58 and 8.59, respectively. At day 90, pH values were 7.54 in CK, 7.68 in BC, 7.50 in FeBC, and 6.90 in ONBC. The mean pH values during the 10–90 d period were 8.06, 8.13, 7.74, and 7.57 for CK, BC, FeBC, and ONBC, respectively. Thus, ONBC maintained higher DO and Eh without causing excessive alkalization, suggesting that its Cd-stabilizing effect was primarily associated with sustained oxygen release and redox regulation rather than a simple pH-driven effect (Fig. 1c).

Together, these results show that oxygen nanobubble loading converted biochar from a mainly passive amendment into an active redox-regulating material. Compared with pristine biochar and

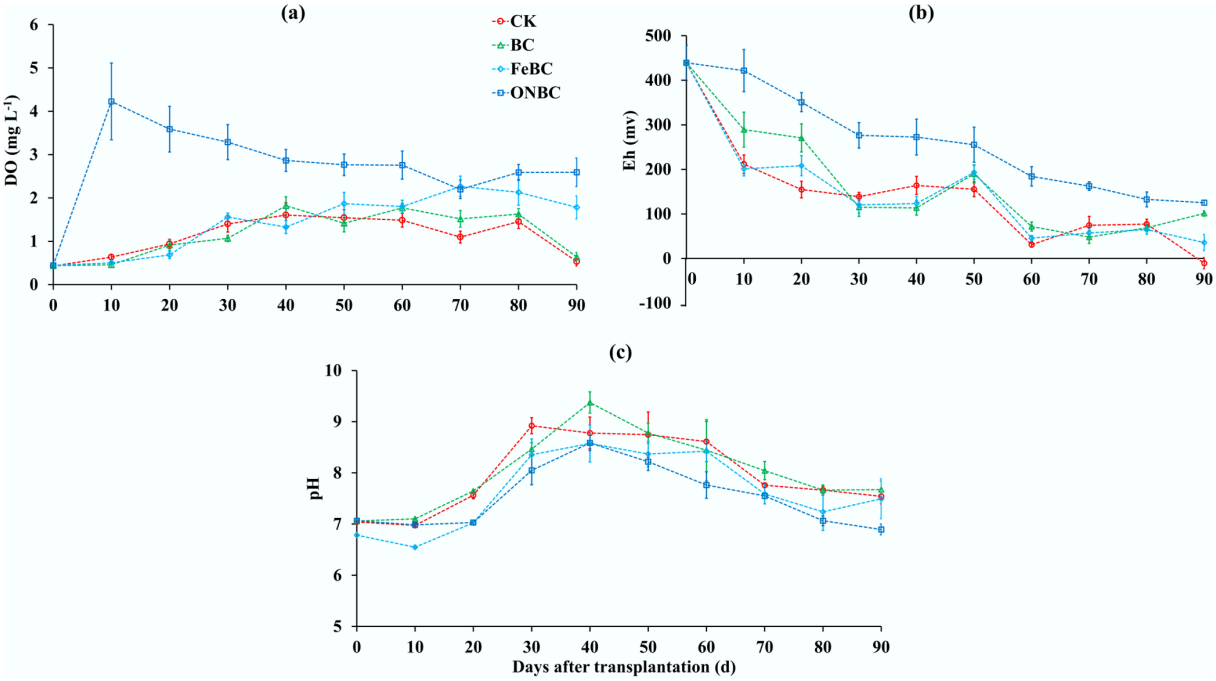

Fig. 1 Effects of different biochar amendments on the flooded rhizosphere environment during rice cultivation. (**a**) Dissolved oxygen (DO) concentration in overlying water; (**b**) rhizosphere redox potential (Eh); and (**c**) soil pH. Data are shown as mean ± standard error ($n = 4$). CK: control without amendment; BC: pristine biochar at 1% (w/w); FeBC: iron-loaded biochar at 1% (w/w); ONBC: oxygen-nanobubble-loaded biochar at 1% (w/w).

Fe-loaded biochar, ONBC maintained higher oxygen availability and a more oxidizing rhizosphere under flooded conditions.

ONBC shifts soil Cd from labile to stable pools

The redox-regulating effect of ONBC was accompanied by a clear redistribution of Cd among soil geochemical fractions (Fig. 2). Exchangeable Cd, the most readily bioavailable fraction, was highest in CK at approximately 0.030 mg kg^{-1}. BC and FeBC reduced exchangeable Cd to approximately 0.027 and 0.022 mg kg^{-1}, respectively, whereas ONBC produced the strongest decrease, lowering exchangeable Cd to approximately 0.009–0.010 mg kg^{-1}. This corresponded to an approximate 67%–70% reduction relative to CK, indicating that ONBC markedly reduced the most mobile Cd pool (Fig. 2a).

Carbonate-bound Cd also decreased strongly under ONBC. The carbonate-bound Cd concentration was approximately 0.110 mg kg^{-1} in CK, 0.100 mg kg^{-1} in BC, and 0.109 mg kg^{-1} in FeBC, but decreased to approximately 0.059 mg kg^{-1} under ONBC. This represented an approximate 46% reduction compared with CK and a reduction of about 41%–46% compared with BC and FeBC (Fig. 2b). Therefore, ONBC reduced both exchangeable and carbonate-bound Cd, indicating a substantial decline in labile Cd fractions.

In contrast, ONBC increased the less mobile Cd fractions. Fe/Mn (hydr)oxide-bound Cd increased from approximately 0.101–0.112 mg kg^{-1} in CK, BC, and FeBC to approximately 0.140 mg kg^{-1} in ONBC (Fig. 2c). Organic matter-bound Cd increased from approximately 0.106–0.109 mg kg^{-1} in the other treatments to approximately 0.157 mg kg^{-1} under ONBC (Fig. 2d). Residual Cd also increased markedly, from approximately 0.104–0.107 mg kg^{-1} in CK, BC, and FeBC to approximately 0.173 mg kg^{-1} under ONBC (Fig. 2e). These increases indicate that ONBC promoted the transformation of Cd into more stable fractions associated with Fe/Mn (hydr)oxides, organic matter, and residual mineral phases.

The percentage distribution of Cd fractions further confirmed this shift. In CK, BC, and FeBC, labile fractions, including exchangeable and carbonate-bound Cd, accounted for approximately 28%–30% of total extracted Cd. Under ONBC, the combined proportion of these labile fractions decreased to approximately 13%. Conversely, the combined proportion of Fe/Mn (hydr)oxide-bound, organic matter-bound, and residual Cd increased to approximately 87% under ONBC, compared with about 70%–72% in the other treatments (Fig. 2f). These results demonstrate that ONBC not only reduced the concentration of labile Cd fractions but also shifted Cd toward more stable soil pools, which is consistent with its ability to maintain higher DO and positive rhizosphere Eh under flooded conditions.

ONBC reduces plant Cd accumulation while increasing IP formation

Both ONBC and FeBC increased Fe concentrations in dithionite-citrate-bicarbonate-extractable IP on rice roots (Fig. 3a), indicating that both

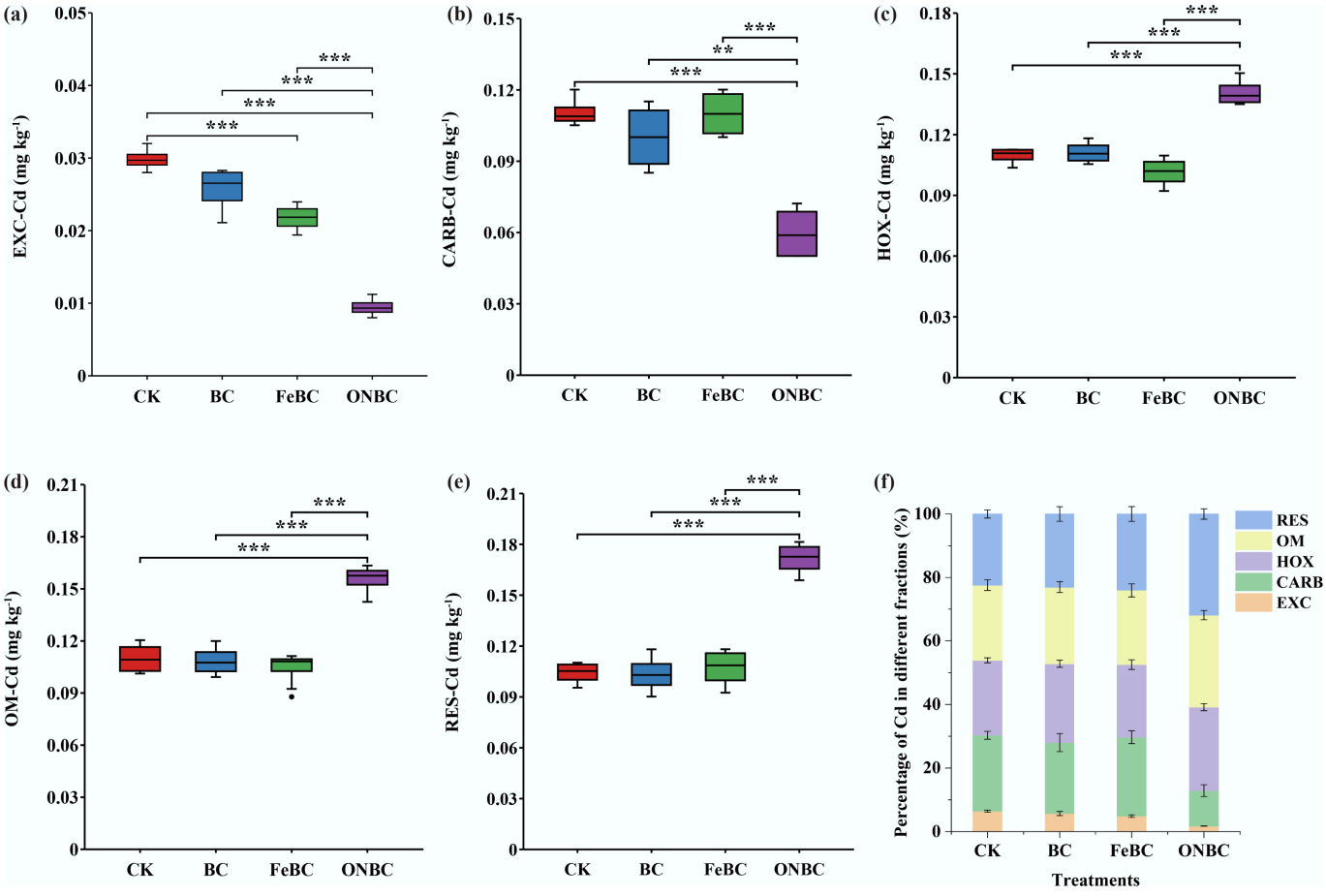

Fig. 2 Effects of ONBC and FeBC amendment on soil Cd speciation: (**a**) exchangeable Cd (EXC); (**b**) carbonate-bound Cd (CARB); (**c**) Fe/Mn (hydr)oxides-bound Cd (HOX); (**d**) organic matter-bound Cd (OM); (**e**) residual Cd (RES); and (**f**) proportion of different Cd fractions in soil. Data are means ± SE (n = 4). Asterisks indicate significant differences (*** $p < 0.001$, ** $p < 0.01$, * $p < 0.05$). CK: control; BC: biochar; FeBC: iron-loaded biochar; ONBC: oxygen-nanobubble-loaded biochar.

https://doi.org/10.48130/bchax-0026-0015

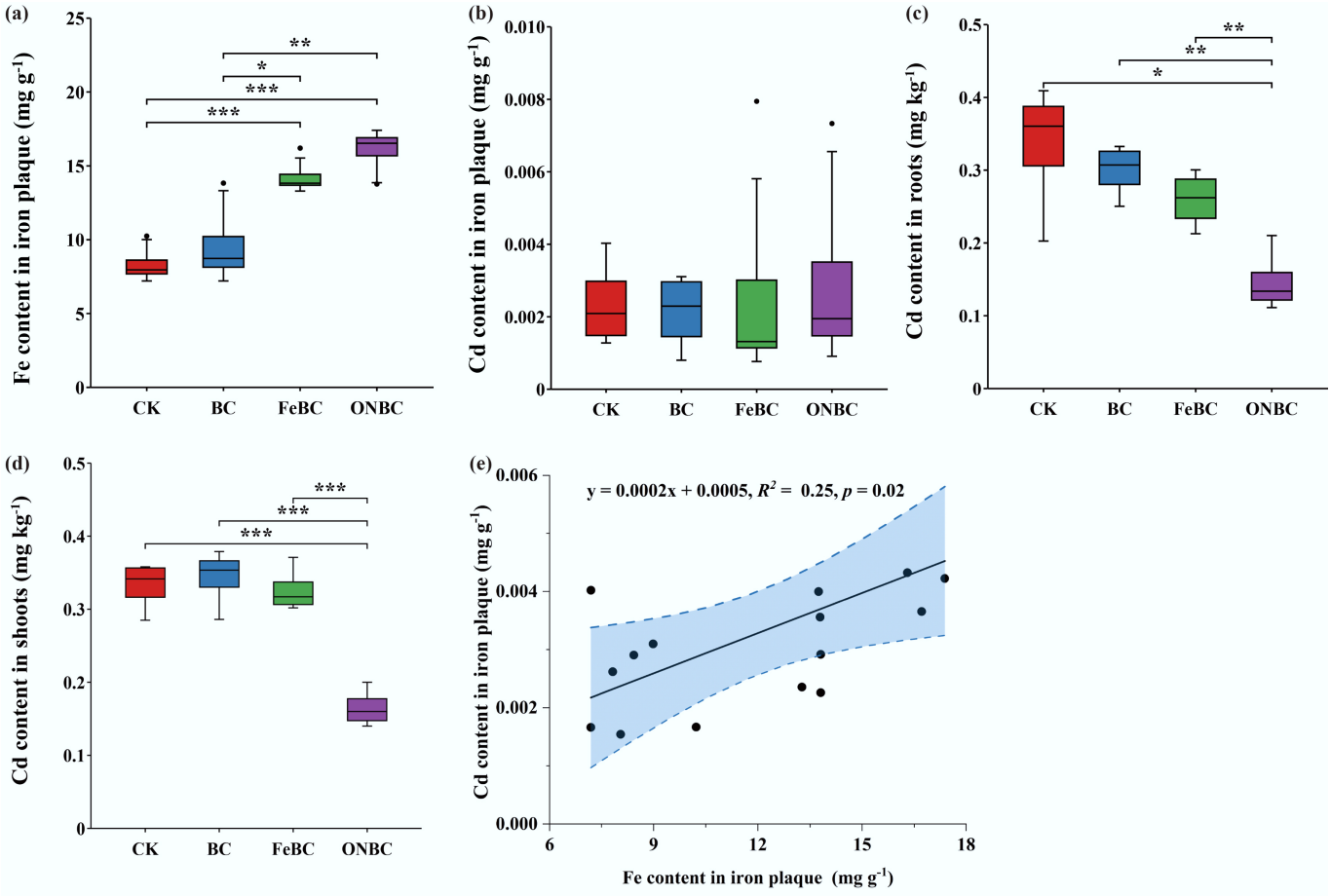

Fig. 3 Effects of the ONBC and FeBC amendment on iron plaque formation and Cd accumulation in rice plants: (**a**) Fe concentration in root iron plaque (extracted by dithionite–citrate–bicarbonate); (**b**) Cd content in root iron plaque; (**c**) Cd concentration in roots; (**d**) Cd concentration in shoots; (**e**) linear regression between Fe and Cd concentrations in root iron plaque. Data are presented as mean ± SE (n = 4). Asterisks indicate significant differences (*** p < 0.001, ** p < 0.01, * p < 0.05). CK: control; BC: biochar; FeBC: iron-loaded biochar; ONBC: oxygen-nanobubble-loaded biochar.

materials promoted plaque formation to some degree. However, Cd retained within the plaque itself did not differ significantly among treatments (Fig. 3b). This suggests that increased plaque abundance was not sufficient on its own to explain the differences in plant Cd.

In contrast, Cd concentrations in rice tissues were clearly lower under ONBC. Root Cd decreased by 2.7-, 2.2-, and 1.9-fold relative to CK, BC, and FeBC, respectively, and shoot Cd decreased by 1.9-, 2.1-, and 2.0-fold, respectively (Fig. 3c, d). Grain Cd was not reported because the rice plants had not reached full grain maturity at harvest, and the available grain material was insufficient for reliable Cd quantification. Therefore, root and shoot Cd concentrations were used as indicators of Cd uptake and translocation during vegetative growth. The weak linear relationship between Fe and Cd in plaque extracts (R^2 = 0.25; Fig. 3e) further indicates that bulk-soil stabilization, rather than direct sequestration of Cd in plaque, was the dominant mechanism by which ONBC lowered plant Cd under the tested conditions.

ONBC restructures the rhizosphere bacterial community

Metagenomic sequencing showed that ONBC also reprogrammed the rhizosphere microbiome (Fig. 4). Rarefaction curves reached saturation, confirming adequate sequencing depth (Supplementary Fig. S1). Relative to CK, BC, and FeBC, ONBC increased the bacterial Chao1 index by 4.3%, 4.1%, and 3.9%, respectively, and increased the Shannon index by 5.6%, 5.2%, and 6.6%, respectively (Fig. 4a, b). OPLS-DA separated ONBC samples clearly from the other treatments at the genus level, and VIP analysis highlighted taxa such as *Pelosinus*, *Pseudooceanicola*, and *Crinalium* among the strongest contributors to treatment separation (Fig. 4c, d).

At the phylum and class levels, the rhizosphere communities were dominated by Pseudomonadota, Actinomycetota, Myxococcota, Bacteroidota, Bacillota, and Cyanobacteriota (Supplementary Figs S2 and S3). The clearest treatment-specific pattern was observed under ONBC, which increased Pseudomonadota and Myxococcota while lowering Actinomycetota. More importantly for Cd immobilization, ONBC enriched several genera associated with Fe/Mn oxidation or transformation, including *Geobacter*, *Rhodopseudomonas*, *Leptothrix*, *Variovorax*, *Pseudomonas*, and *Acinetobacter* (Fig. 4e, f). These shifts support the view that ONBC stimulated an oxidative microbial network capable of reinforcing redox-sensitive mineral formation around roots.

ONBC enriches microbial functions linked to Cd detoxification and nutrient turnover

To elucidate microbial mechanisms potentially involved in Cd stabilization, we analyzed functional genes associated with bacterial Cd resistance and detoxification (Fig. 5; Supplementary Table S3).

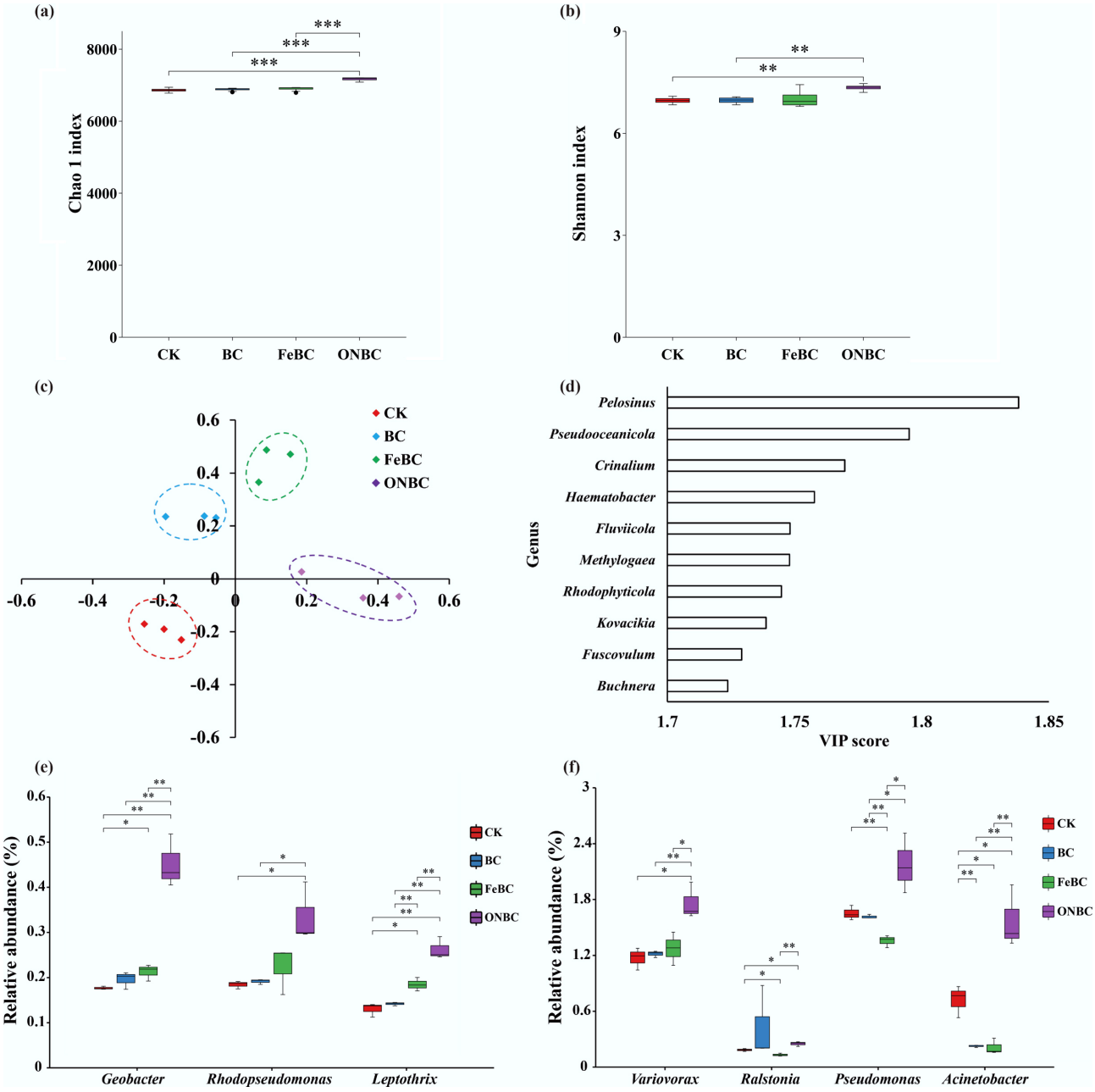

Fig. 4 Effects of the ONBC and FeBC amendments on soil bacterial community diversity and structure: (**a**) Chao1 index; (**b**) Shannon index; (**c**) OPLS-DA loading plot; (**d**) variable importance in projection (VIP) scores for the top 10 genera; (**e**) relative abundance of Fe -oxidizing genera; and (**f**) relative abundance of Mn-oxidizing genera. Data are mean ± SE (n = 4). Asterisks indicate significant differences (*** $p < 0.001$, ** $p < 0.01$, * $p < 0.05$). CK: control; BC: biochar; FeBC: iron-loaded biochar; ONBC: oxygen-nanobubble-loaded biochar.

These genes were grouped into four processes: Cd^{2+} influx transport, Cd^{2+} efflux, cytoplasmic Cd^{2+} detoxification, and Cd^{2+} sensing and binding (Fig. 5a). In Fig. 5, the subfigures are arranged to first present the overall Cd^{2+} stabilization pathway, followed by membrane transport processes, including Cd^{2+} influx and efflux, and then intracellular detoxification and stress-response processes.

Both FeBC and ONBC significantly reduced the abundance of Cd^{2+} influx transporter genes (*ZupT* and *MntH*) relative to CK and BC (Fig. 5b). In contrast, ONBC markedly increased the abundance of Cd^{2+} efflux transporter genes, including *ZntA*, *CusA*, *CusB*, and *CusC* (Fig. 5c), consistent with enhanced microbial capacity to export intracellular Cd. FeBC also affected some of these genes, but the response was weaker and less consistent than that under ONBC.

For cytoplasmic detoxification, ONBC significantly increased the abundance of *CueO*, *GshA*, *GshB*, and *GorA* (Fig. 5d), genes associated with glutathione metabolism and cellular redox homeostasis. ONBC also upregulated genes involved in Cd^{2+} sensing and binding, including *CusA*, *CusB*, *GroEL*, and *DnaK*, while slightly downregulating *CadC* (Fig. 5e). FeBC increased *GshB* and *GorA* to a lesser extent than ONBC. Together, these patterns indicate that ONBC activated a coordinated microbial Cd-defense response, characterized by reduced Cd^{2+} influx, enhanced Cd^{2+} efflux, stronger cytoplasmic detoxification, and improved Cd^{2+} sensing/binding capacity.

Overall, ONBC activated a broader network of genes involved in microbial Cd defense than FeBC. The concurrent suppression of influx genes and stimulation of efflux, detoxification, and binding

https://doi.org/10.48130/bchax-0026-0015

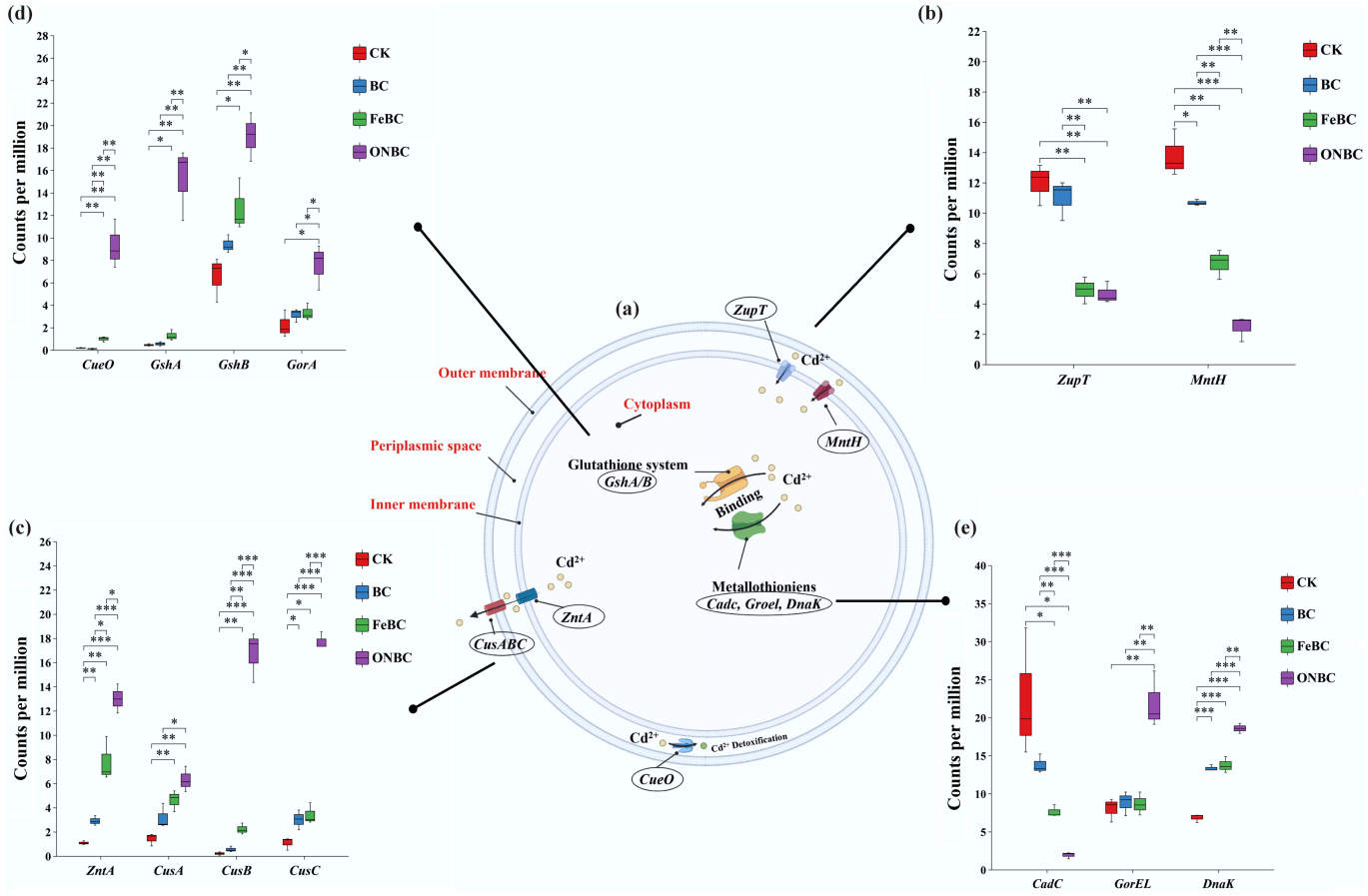

Fig. 5 Effects of different biochar amendments on bacterial genes involved in Cd^{2+} stabilization and detoxification pathways. (**a**) Schematic overview of bacterial Cd^{2+} stabilization pathways. The panels are organized from the overall pathway to membrane transport processes and then intracellular detoxification/stress-response processes. (**b**) Cd^{2+} influx transporter genes, including *ZupT* and *MntH*. (**c**) Cd^{2+} efflux transporter genes, including *ZntA*, *CusA*, *CusB*, and *CusC*. (**d**) Cytoplasmic Cd^{2+} detoxification genes, including *CueO*, *GshA*, *GshB*, and *GorA*. (**e**) Cd^{2+} sensing and binding genes, including *CadC*, *CusA*, *CusB*, *GroEL*, and *DnaK*. Data are shown as mean ± standard error. Asterisks indicate significant differences among treatments (* $p < 0.05$, ** $p < 0.01$, *** $p < 0.001$). CK: control without amendment; BC: pristine biochar; FeBC: iron-loaded biochar; ONBC: oxygen-nanobubble-loaded biochar.

genes is consistent with reduced microbial Cd stress in the ONBC-treated rhizosphere.

ONBC stimulates microbial functional genes involved in nutrient turnover and redox cycling

To clarify how ONBC and FeBC amendments influenced soil microbial functions potentially related to Cd retention and nutrient turnover, we analyzed genes associated with C mineralization, N mineralization, P mineralization, and Fe–S–Mn redox cycling using z-score-normalized heatmaps (Fig. 6; Supplementary Tables S4–S7).

The heatmap revealed that ONBC markedly enriched multiple C-turnover modules (Fig. 6a). Genes involved in polysaccharide degradation (*celB*, *bglX*, *xynA*, *amyA*, and *pulA*), central carbon metabolism (*hk, gltA, icd, sucA*), fatty-acid catabolism (*lip, acd, fadB, echA*), and aromatic compound degradation (*pcaG, pcaH, benA, benB*) all increased under ONBC. These patterns are consistent with greater microbial respiration and organic matter turnover under the more oxic conditions created by ONBC. In contrast, FeBC produced only modest or scattered increases in core C-mineralization genes.

ONBC also broadly increased genes involved in organic N depolymerization and deamination (Fig. 6b), including protease/peptidase genes (*aprE*, *pepN*, *pepA*, *nprE*, *npr*), deaminases (*mao*, *aoc2*, *LeuDH*, *ald*, *ansA*, *aspA*), amino-sugars and chitin turnover genes (*chiA*, *cda*, *nagB*), and ureases (*ureA*, *ureB*, *ureC*). These responses indicate greater potential for conversion of organic N to mineral N under ONBC. FeBC had weaker effects on N-mineralization genes, with only limited increases (e.g., *sdaK*, *LeuDH*), consistent with less pronounced oxygenation.

Likewise, genes associated with P-mineralization were enriched under ONBC (Fig. 6c). ONBC increased genes involved in organic P hydrolysis (*phoA*, *pho*, *aphA*, *phoN*, and *ppa*), phytase-mediated P release (*appA*), nucleic acids P turnover (*ushA*, *ppx1*), phosphonate utilization (*phnI*, *phnG*, *phnA*), and P-regulatory components (*phoB*, *phoR*, *phoU*). This pattern indicates greater potential for microbial P turnover and for the generation of phosphate that may participate in Cd immobilization. By contrast, FeBC reduced several P-mineralization genes relative to BC and CK, including *phyA*, *appA*, *HisB*, *yfbR*, *pde*, *ppx1*, *phnL*, *phnI*, *phnH*, *phnA*, and *phnX*.

Genes involved in Fe, S, and Mn redox cycling also responded strongly among treatments (Fig. 6d). ONBC increased genes associated with oxidative Fe/Mn pathways, including *fth1*, *sod2*, *katE*, multicopper oxidases (*mco*, *moxa*, *mnxG*, *mcoA*), and cytochrome c oxidase subunits (*ccoN*, *ccoO*, *ccoP*, *ccoQ*), while decreasing S-reduction/oxidation markers (*aprA*, *aprB*, *dsrA*, *dsrB*) and Fe-reductase/regulatory genes (*yqjH* and *feR*). FeBC, in contrast, increased a suite of S- and Fe-related genes, including *aprA*, *aprB*, *dsrA*, *dsrB*, *sat*, *tst*, *sdo,* and Fe-handling regulators/storage, including *yqjH*, *feR*, *fth1*, and *bfr*. These contrasting profiles suggest that

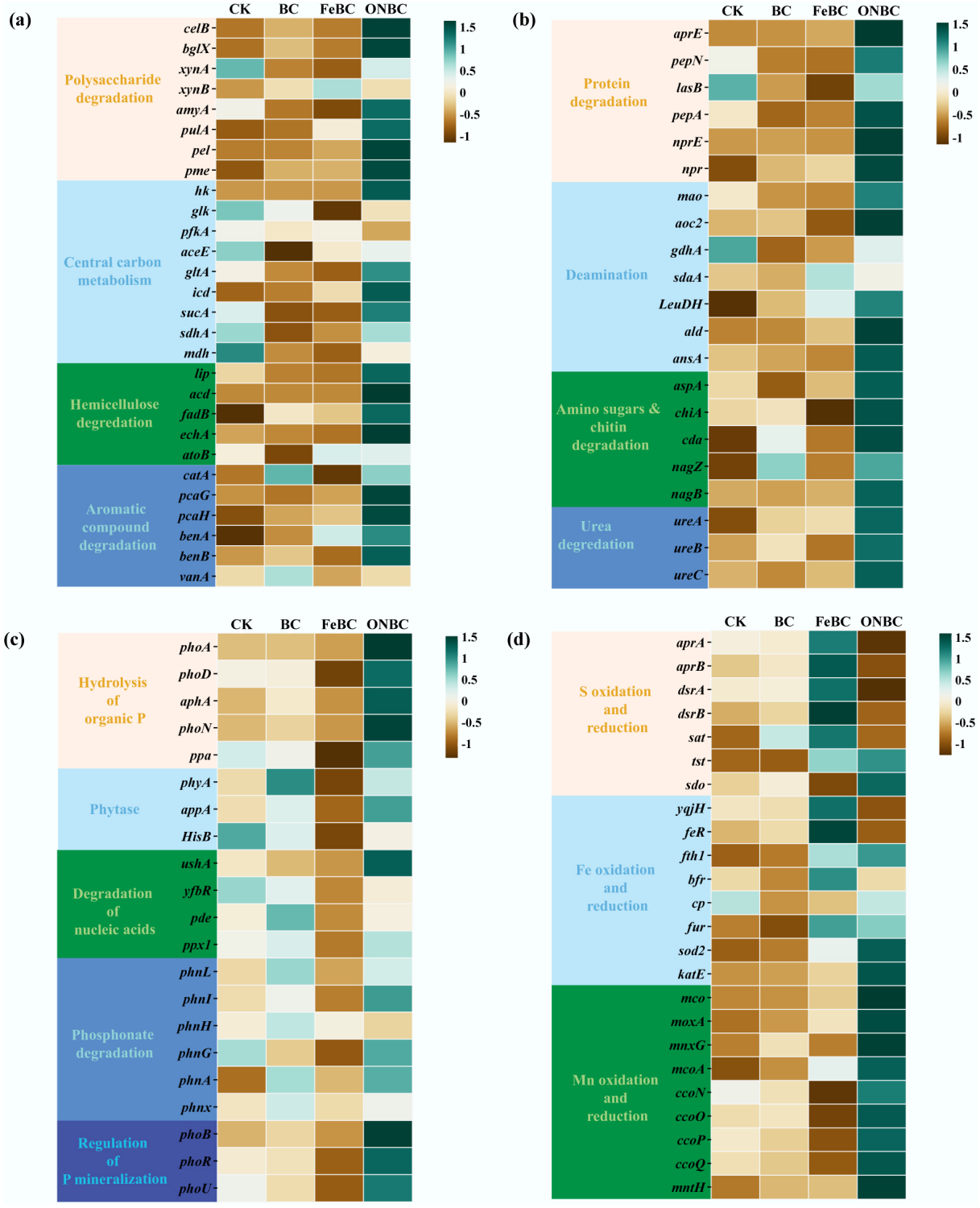

Fig. 6 Heatmap of differentially abundant microbial functional genes in paddy soils in response to FeBC and ONBC amendments. Functional genes are grouped into four categories: (**a**) C mineralization; (**b**) N mineralization; (**c**) P mineralization; and (**d**) Fe–S–Mn redox cycling. Relative abundances are shown as z-score-normalized counts per million (CPM) from metagenomic analysis. Gene abbreviations correspond to full names and EC numbers listed in Supplementary Tables S3–S7. CK: control; BC: biochar; FeBC: iron-loaded biochar; ONBC: oxygen-nanobubble-loaded biochar.

ONBC favored oxidative Fe/Mn pathways, whereas FeBC favored Fe/S transformations.

Complementing these specific functional genes in Fig. 6, the broader functional profile of the microbial communities was further evaluated from KEGG metabolic pathway abundances (Supplementary Fig. S4). Pathways clustered clearly by treatment, with ONBC showing the highest relative abundances for oxidative phosphorylation, which supports enhanced ATP production under oxygenated conditions, carbon fixation in prokaryotes, N metabolism, and S metabolism. These patterns are consistent with enhanced energy metabolism and nutrient turnover under oxygenated conditions. FeBC displayed intermediate enrichment for S metabolism and

energy metabolism pathways but lower abundances for pathways such as glycolysis/gluconeogenesis and amino acid biosynthesis, indicating a narrower metabolic response. CK and BC generally showed baseline or lower pathway abundances, consistent with limited oxygenation and weaker microbial activation. Overall, these results indicate that ONBC broadly activated rhizosphere microbial functions related to nutrient turnover and oxidative redox cycling.

ONBC improves plant growth and root physiological traits

The microbial functional changes induced by ONBC coincided with improved rice growth and root physiological performance (Figs 7 and 8). Compared with CK, ONBC increased whole-plant fresh biomass by 44.7%, indicating that oxygen nanobubble loading alleviated growth limitation under Cd-contaminated flooded conditions. Root morphological traits were also improved under ONBC, with root diameter and root volume reaching the highest values among all treatments (Fig. 7). These responses suggest that ONBC promoted root development and overall plant growth more effectively than pristine biochar or Fe-loaded biochar did.

Root physiological and antioxidant responses further supported the beneficial effect of ONBC. ONBC increased root activity by 64.5% and SOD activity by 85.4% relative to CK, indicating enhanced root metabolic activity and stronger antioxidant defense under ONBC treatment (Fig. 8). In contrast, FeBC suppressed several growth and physiological traits, and CAT activity was lowest under FeBC. Taken together, these plant responses suggest that ONBC improved rice growth and root function, likely by reducing Cd stress and creating a more favorable rhizosphere environment.

Integrated pathways support a redox-microbiome mechanism for Cd stabilization

The SEM clarified how ONBC amendment cascades through soil–plant–microbe linkages to suppress Cd accumulation and promote rice growth. Model fit indices (GFI, SRMR) indicated an acceptable fit, and significant paths are shown in Fig. 9. ONBC exerted a strong direct effect on the rhizosphere redox environment (higher DO/Eh) and on microbial functions, which together shifted soil Cd speciation from labile pools toward more stable fractions. In turn, the enrichment of Fe/Mn (hydr)oxide-bound Cd and organic/residual pools was negatively associated with plant Cd, indicating effective immobilization within soil matrices. By contrast, root IP showed only a weak, non-significant link to plant Cd (Fig. 9a), consistent with the poor Fe–Cd correlation in plaques (Section 'ONBC shifts soil Cd from labile to stable pools'). Parallel microbial routes were evident: ONBC positively influenced Cd-detoxification gene modules (efflux/detox/sensing), which collectively reinforced the shift toward less bioavailable Cd forms and further reduced plant Cd. Downstream, plant Cd was

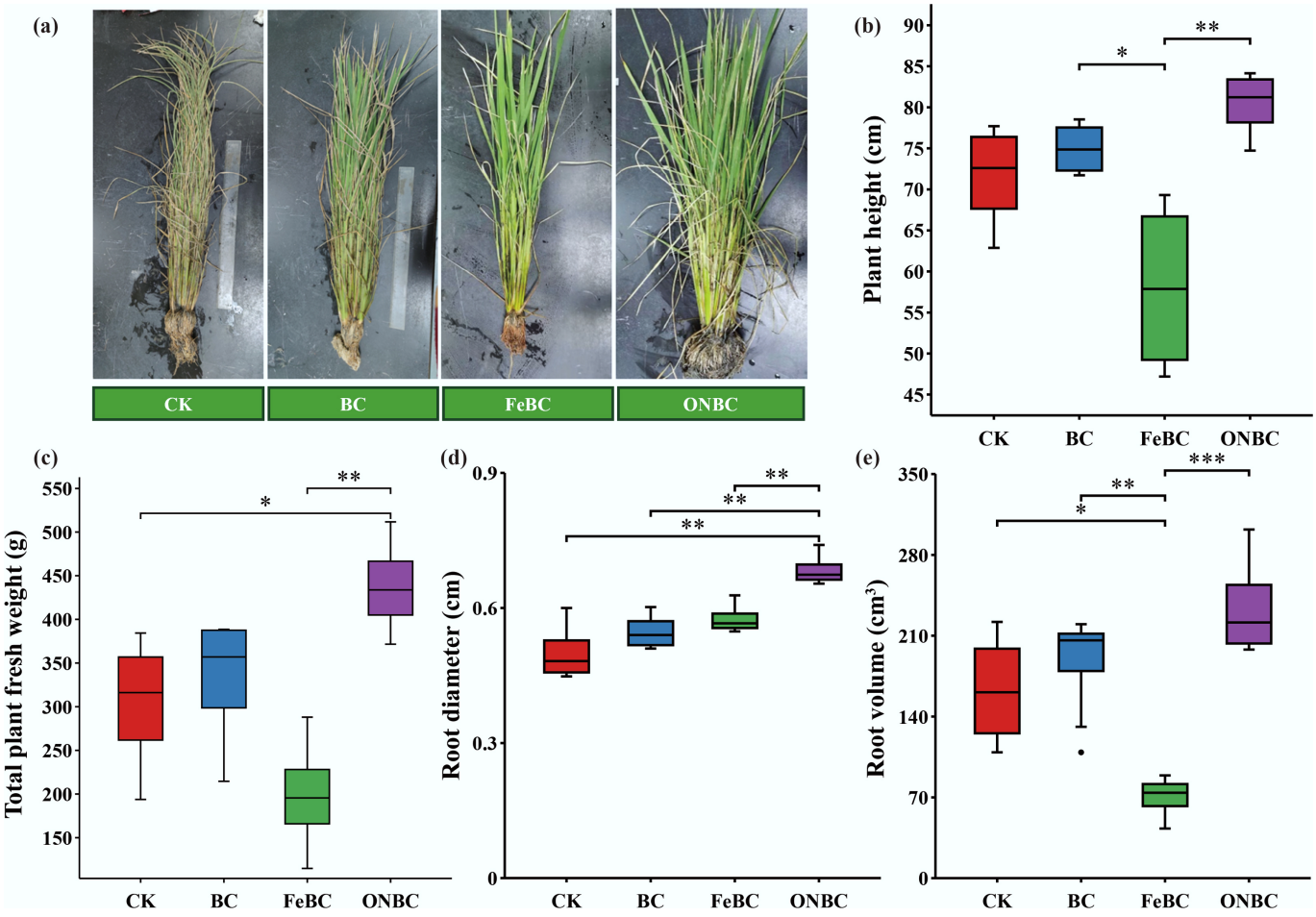

Fig. 7 Effects of the ONBC and FeBC on rice plant growth performance: (**a**) photographs at harvest; (**b**) plant height; (**c**) fresh weight of whole plant; (**d**) root diameter, and (**e**) root volume. Data are mean ± SE (n = 4). Asterisks denote significance (*** $p < 0.001$, ** $p < 0.01$, * $p < 0.05$). CK: control; BC: biochar; FeBC: iron-loaded biochar; ONBC: oxygen-nanobubble-loaded biochar.

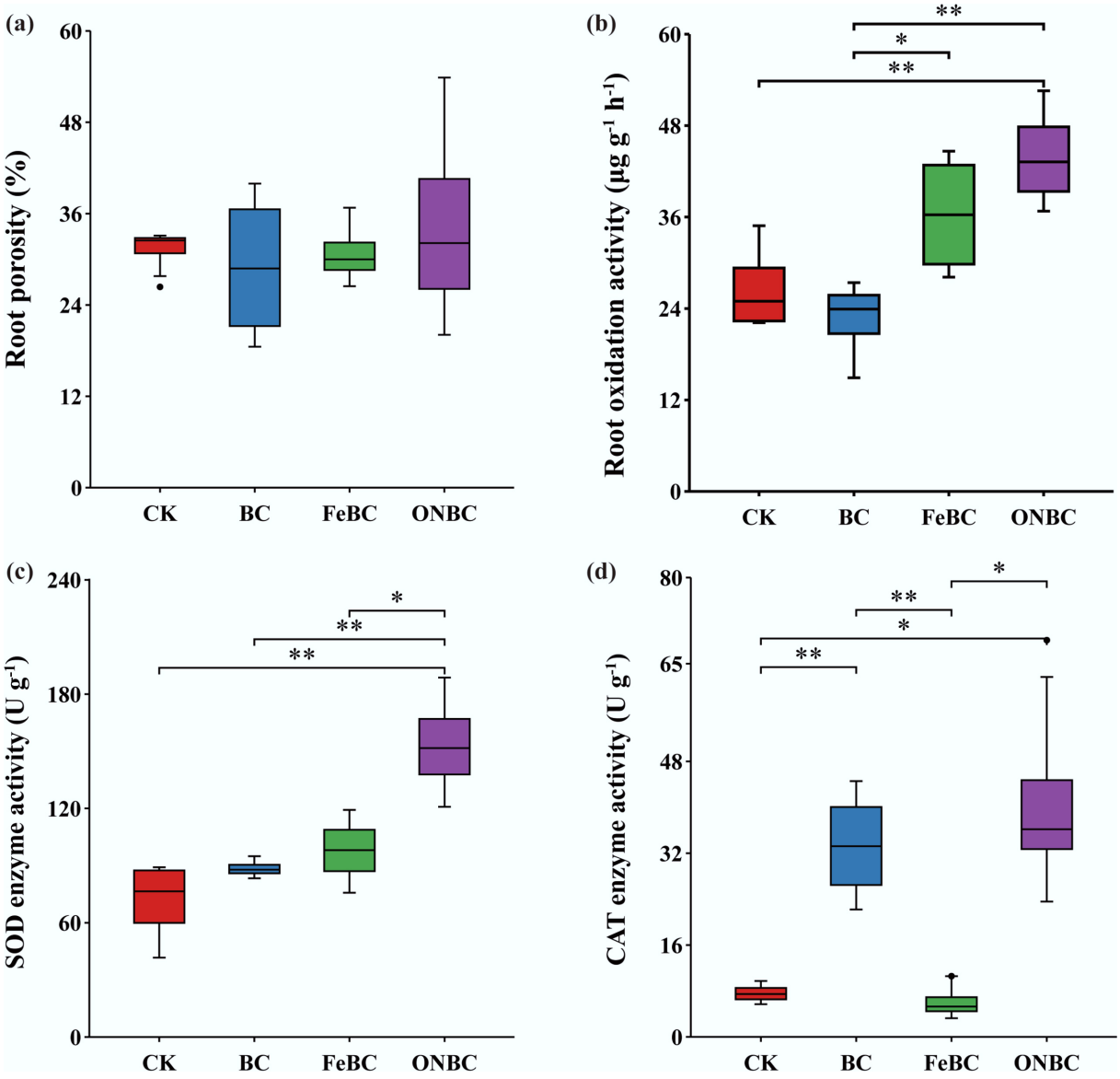

Fig. 8 Root physiological and biochemical responses of rice to ONBC and FeBC amendments: (**a**) root porosity; (**b**) root oxidative activity; (**c**) superoxide dismutase (SOD) activity; and (**d**) catalase (CAT) activity. Data are presented as mean ± SE (n = 4). Asterisks indicate significant differences (*** $p < 0.001$, ** $p < 0.01$, * $p < 0.05$). CK: control; BC: biochar; FeBC: iron-loaded biochar; ONBC: oxygen-nanobubble-loaded biochar.

negatively associated with growth performance, whereas ONBC also showed a positive, indirect path to growth via enhanced nutrient-mineralization functions (C/N/P) and root activity, aligning with observed gains in biomass and root traits (Fig. 9b). Overall, these results support a model in which ONBC primarily reduced plant Cd through redox- and microbiome-driven changes in soil Cd speciation.

Discussion

ONBC promotes rice growth and mitigates Cd uptake through sustained redox regulation and Fe/Mn (hydr)oxides formation

The stronger reduction in plant Cd uptake under ONBC is consistent with its capacity to maintain more oxidizing conditions in flooded soil. Relative to BC and FeBC, ONBC sustained higher DO and positive Eh throughout cultivation, conditions that favor repeated oxidation of Fe^{2+} and Mn^{2+} and the formation of reactive Fe/Mn (hydr)oxides. These phases can retain Cd through adsorption, coprecipitation, and surface complexation[19,20]. Additionally, ONB-derived interfacial reactive oxygen species (•OH, $^1O_2$) further accelerate Fe^{2+} oxidation and organic matter degradation[14,20], fostering a self-sustaining 'sink' for Cd around rice roots. Accordingly, ONBC shifted Cd from exchangeable and carbonate-bound pools to Fe/Mn (hydr)oxide-bound, organic, and residual fractions. Pristine biochar can immobilize Cd through sorption and pH effects, but in flooded systems it does not provide the sustained redox control observed for ONBC[12,13].

Higher DO and Eh also promoted IP formation on rice roots. Both ONBC and FeBC significantly increased Fe accumulation in root IP, consistent with prior reports that oxygen enrichment or Fe supplementation stimulates IP development[21,22]. However, Cd concentrations in the IP were similar among treatments, and the relationship between Fe and Cd was weak (Fig. 4e). These observations suggest that, in this system, IP was not the dominant sink for Cd, although IP acts as a more effective barrier for other heavy metals[23]. This divergence may arise from varying affinities of amorphous vs

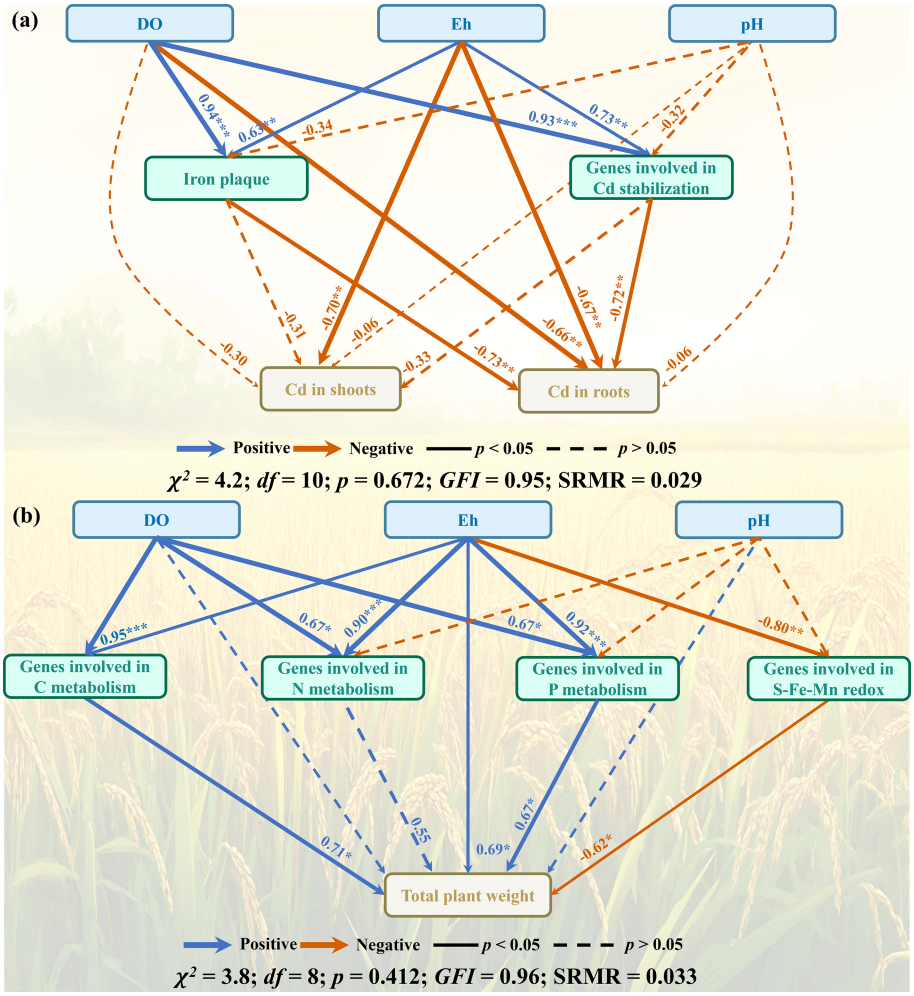

Fig. 9 SEM analysis illustrating the pathways by which ONBC influenced (**a**) Cd accumulation in rice plants, and (**b**) plant growth. Solid and dashed arrows indicate significant and nonsignificant relationships, respectively. Blue arrows indicate positive relationships and orange arrows indicate negative relationships. Numbers adjacent to arrows are path coefficients. Significance levels are * $p < 0.05$, ** $p < 0.01$, and *** $p < 0.001$. GFI: goodness-of-fit index; SRMR: standardized root mean squared residual.

crystalline Fe (hydr)oxides for specific metals, as well as competition from other ions in the soil matrix[4,9,10]. Instead, bulk-soil immobilization appears to have been more important for reducing Cd transfer to the plant.

The contrast between ONBC and FeBC further emphasizes the importance of sustained oxygen supply. ONBC's micro-oxygenation maintains higher Eh, enabling repeated Fe/Mn oxidation cycles and preventing Cd remobilization[7,8]. In contrast, FeBC supplies exogenous Fe^{3+} but lacks ongoing oxygenation, potentially leading to transient Fe(III) reduction in anaerobic microsites and subsequent Cd release[21,22,24]. Evidence from analogous Fe-modified biochars, such as nanoscale zero-valent iron-loaded variants, shows that while they increase soil pH and available Fe, they can variably alter Cd fraction and inhibit microbial enzymes without sustained oxygen[12,21]. However, without sustained oxygen, FeBC fails to sustain the oxidative cycles necessary for persistent Cd immobilization, underscoring oxygen as the pivotal factor. Thus, dynamic Fe/Mn redox cycling—driven by nanobubble-mediated O_2 release—integrates geochemical stabilization with biotic regulation for persistent Cd immobilization.

This reduced Cd toxicity directly contributed to improved rice growth under ONBC, as evidenced by taller shoots, denser canopies, greener leaves, higher biomass, thicker roots, and greater root volume compared with controls. Enhanced root activity and antioxidant defenses likely bolstered resilience against residual Cd-induced oxidative stress, while sustained oxygenation supported efficient nutrient uptake and alleviated impairments in photosynthesis and metabolism[11,18]. Conversely, FeBC suppressed growth parameters and CAT activity, indicating potential Fe-induced oxidative imbalance or secondary stress[21,24]. These findings underscore ONBC's superiority in balancing Cd mitigation with plant vigor in contaminated paddies, outperforming traditional biochar amendments that may enhance growth but often fail to address redox-sensitive Cd dynamics as effectively[11,21,25].

ONBC reshapes the rhizosphere microbiome and functional gene networks

In addition to its geochemical effects, ONBC restructured the rhizosphere microbiome. ONBC increased bacterial diversity and enriched taxa associated with oxidative metabolisms, including Fe- and Mn-oxidizing genera. At higher taxonomic levels, ONBC enriched Pseudomonadota and Myxococcota while reducing Actinomycetota, aligning with oxygen-driven selections observed in similar systems[11]. Key enrichments in Fe/Mn-oxidizing genera (e.g., *Leptothrix*, *Geobacter*,

Rhodopseudomonas, *Pseudomonas*, *Acinetobacter*) facilitate oxide formation through extracellular electron transfer and multicopper oxidases[20,26,27], enhancing Cd sorption onto biogenic Fe/Mn (hydr)oxides[19,20]. This microbial mediation complements abiotic redox processes, aligning with observations in ONB-loaded systems for arsenic mitigation[28], where similar microbial shifts reduced heavy metal translocation by promoting oxidative barriers[14].

At the genetic level, ONBC suppressed Cd influx transporters (*ZupT*, *MntH*)[29] while upregulating efflux systems (*ZntA*, *CusA/B/C*)[30,31], detoxification genes (*CueO*, *GorA*, *GshA/B*)[32,33], and sensing/binding pathways (*CusA/B*, *GorE1*, *DnaK*)[32,33] (Fig. 6). This coordinated response reduces intracellular Cd toxicity by enhancing export and sequestration, with stronger effects under ONBC than FeBC, suggesting that oxygen-driven metabolic activation fosters microbial resilience[18,32].

Furthermore, ONBC stimulates nutrient cycling genes, boosting C mineralization, N depolymerization, and P hydrolysis. These enhancements liberate bioavailable nutrients, improving rice uptake and forming Cd-phosphate precipitates[33], while also aligning with broader KEGG pathway shifts toward energy and metabolism. In contrast, FeBC amplifies Fe–S–Mn redox genes but dampens P mineralization, possibly due to phosphate sorption on Fe phases[21,22,34]. This highlights a trade-off: FeBC favors reductive Fe–S coupling for sulfide precipitation, similar to the studies where Fe-enriched biochars reduced heavy metal bioavailability via microbial S cycling but at the cost of nutrient limitations[23].

Taken together, the microbial data indicate that ONBC did not act solely as a chemical amendment. Rather, it shifted the rhizosphere toward a functionally distinct microbiome with greater potential for nutrient turnover, oxidative redox cycling, and Cd detoxification, which is consistent with the stronger reduction in plant Cd observed under this treatment.

Implications, limitations, and future perspectives for paddy-soil remediation

Given the widespread Cd contamination in Chinese farmlands (affecting ~1.3×10^5 ha and yielding 5.0×10^4 tons of contaminated rice annually)[35,36], ONBC emerges as a promising, energy-efficient alternative to traditional aeration, pristine biochar, or Fe modifications. ONBC reduced Cd accumulation in roots and shoots and may contribute to lowering Cd transfer risk in rice production systems, although direct grain Cd assessment at full maturity is needed. Because the material is produced from crop-residue biochar and delivers oxygen without energy-intensive field aeration, it offers a practical route toward resource-efficient remediation and safer rice production in flooded paddies, where redox fluctuations exacerbate Cd mobility[7,8].

This work demonstrates that a residue-derived biochar can be engineered to deliver a functional redox service in flooded soil. The material does not immobilize Cd solely through adsorption; rather, it orchestrates a sequence of environmental responses—oxygen retention, redox stabilization, oxidative Fe/Mn cycling, microbial detoxification, and nutrient turnover—that collectively suppress Cd bioavailability. This systems-level mechanism broadens the design space for carbonaceous remediation materials.

From a remediation perspective, ONBC is promising because it is based on crop-residue biochar and avoids the energy demand of continuous field aeration. The concept may also be relevant to other redox-sensitive contaminants in flooded soils and sediments. However, this study remains a greenhouse pot experiment conducted in a single soil at a single application rate. Field validation is required to determine scalability, oxygen-retention durability, cost-effectiveness, and performance across soil types, cultivars, and water-management regimes. Future work should also refine material characterization, especially oxygen-release kinetics and surface/interfacial properties, and pair remediation performance with techno-economic and life-cycle assessment.

From a preliminary cost perspective, ONBC production mainly involves the parent biochar, oxygen gas, and energy consumption during vacuum-pressure loading, without the use of expensive chemical oxidants or additional metal salts. At the tested application rate of 1% (w/w), the field-equivalent material demand for incorporation into the 0–20 cm plow layer would be approximately 20–30 t ha^{-1}, depending on soil bulk density. Therefore, the parent biochar and field application cost are expected to be the major cost components, whereas oxygen loading represents an additional but relatively simple processing step. Considering its simultaneous effects on Cd immobilization, rhizosphere oxygenation, and plant growth improvement, ONBC may have practical value for high-risk Cd-contaminated paddy soils. However, future field studies should further optimize the application rate and conduct a complete cost–benefit analysis including material production, transport, field application, grain Cd reduction, and yield response.

Despite these implications, several limitations should be acknowledged. This study was conducted under greenhouse pot conditions using a single Cd-contaminated paddy soil, one rice variety, one contamination level, and one ONBC application rate; therefore, extrapolation to field conditions requires further verification. In real paddy systems, soil properties, Fe/Mn oxide abundance, irrigation and drainage regimes, seasonal redox dynamics, and cultivar-dependent Cd uptake may all affect ONBC performance. In addition, the effect of ONBC depends on sustained oxygen release from the biochar matrix. Although the higher DO and Eh observed under ONBC provided functional evidence of oxygen release, the oxygen-loading amount, release rate, release duration, and oxygen loss during storage were not fully characterized. Future studies should quantify ONBC oxygen-loading and release kinetics, evaluate storage stability, and conduct multi-soil, multi-cultivar, multi-rate field trials to verify grain Cd reduction, crop yield, and long-term remediation performance.

Conclusion

ONBC functioned as an engineered carbonaceous platform for Cd stabilization in flooded paddy soil. Relative to pristine biochar and FeBC, ONBC sustained oxic rhizosphere conditions, shifted Cd from labile to stable geochemical pools, reduced Cd accumulation in rice tissues, and enriched microbial functions associated with oxidative Fe/Mn cycling and Cd detoxification. The mechanistic evidence indicates that oxygen loading transformed biochar from a passive sorbent into an active redox-regulating material. Bulk-soil immobilization driven by coupled redox and microbiome responses was the dominant pathway, whereas IP made a smaller contribution to plant Cd reduction under the conditions tested. These findings position ONBC as a promising design strategy for carbon-based remediation in flooded environments. Before submission and eventual publication, the material concept should be further strengthened with field validation, improved reporting of oxygen-retention behavior, and a public repository for metagenomic data.

Supplementary information

It accompanies this paper at: https://doi.org/bchax-0026-0015.

Ethical statements

In this paper, all the writing, scientific content, data interpretation, and conclusions were developed solely by the authors.

Author contributions

The authors confirm their contributions to the paper as follows: Qingnan Chu: data curation, visualization, writing – original draft; Detian Li: investigation, methodology; Shuhan Xu: conceptualization, investigation; Dongrong Pan: investigation, methodology; Haoyu Cao: investigation, methodology; Hui Gao: investigation, methodology; Chengming Zhang: data curation, visualization; Shanliang Liu: data curation, visualization; Bin Liu: investigation, methodology; Wenjia Chen: investigation, methodology; Qiuyue Wang: investigation, validation; Jinghua Wu: investigation, validation; Ping He: resources, writing – review and editing; Zhimin Sha: funding acquisition, supervision, writing – review and editing. All authors reviewed the results and approved the final version of the manuscript.

Data availability

The datasets generated during and/or analyzed during the current study are available from the corresponding author on reasonable request.

Funding

The authors would like to acknowledge funding from the Shanghai Agricultural Applied Technology Development Program, China (A2025001), and the 2025 Shanghai Municipal Grassroots Science Popularization Action Plan Project (JCKP2025-29).

Declarations

Competing interests

The authors declare that they have no known competing financial interests or personal relationships that could have appeared to influence the work reported in this paper.

Author details

[1]School of Agriculture and Biology, Shanghai Jiao Tong University, 800 Dongchuan Road, Shanghai 200240, China; [2]Australian Rivers Institute and School of Environment and Science, Griffith University, Brisbane, QLD 4111, Australia; [3]College of Chemistry and Life Sciences, Sichuan Philosophy and Social Key Laboratory of Monitoring and Assessing for Rural Land Utilization, Chengdu Normal University, Haike Road-99 East Section, Chengdu 611130, China; [4]SEEK Biotechnology (Shanghai) Co., Ltd, Shanghai 200240, China; [5]Qingpu District Agro-Technology Extension Service Center, 60 Qingkun Road, Qingpu District, Shanghai 201799, China; [6]Qingpu Modern Agricultural Development Zone, Shanghai 200240, China; [7]Institute of Agricultural Resources and Regional Planning, Chinese Academy of Agricultural Sciences, Beijing 100081, China

References

[1] Zhang N, Lv C, Li Y, Panagos P, Ballabio C, et al. 2025. Geochemical-integrated machine learning approach predicts the distribution of cadmium speciation in European and Chinese topsoils. *Communications Earth & Environment* 6:548

[2] Zhou JW, Li Z, Liu MS, Yu HM, Wu LH, et al. 2020. Cadmium isotopic fractionation in the soil–plant system during repeated phytoextraction with a cadmium hyperaccumulating plant species. *Environmental Science & Technology* 54:13598−13609

[3] Ali W, Mao K, Zhang H, Junaid M, Xu N, et al. 2020. Comprehensive review of the basic chemical behaviours, sources, processes, and endpoints of trace element contamination in paddy soil-rice systems in rice-growing countries. *Journal of Hazardous Materials* 397:122720

[4] Li Y, Tao H, Cao H, Wan X, Liao X. 2024. Achieving synergistic benefits through integrated governance of cultivated cadmium contamination via multistakeholder collaboration. *Nature Communications* 15:9817

[5] Lin XY, Li HB, Juhasz AL, Jiao DD, Zhou L, et al. 2025. Lower cadmium bioavailability and toxicity in japonica rice than in indica rice: mechanisms and health implications. *Environmental Science & Technology* 59:1156−1169

[6] Yang Y, Zhang Y, Zhou Q, Gu Y, Yao Y. 2024. Urinary cadmium levels in China (1982–2021): regional trends and influential factors. *Environmental Research* 251:118618

[7] Zhao FJ, Wang P. 2020. Arsenic and cadmium accumulation in rice and mitigation strategies. *Plant and Soil* 446:1−21

[8] Wang Z, Tu S, Shehzad K, Hou J, Xiong S, et al. 2025. Comparative study of organosilicon and inorganic silicon in reducing cadmium accumulation in wheat: insights into rhizosphere microbial communities and molecular regulation mechanisms. *Journal of Hazardous Materials* 492:138061

[9] Li H, Zheng X, Tao L, Yang Y, Gao L, et al. 2019. Aeration increases cadmium (Cd) retention by enhancing iron plaque formation and regulating pectin synthesis in the roots of rice (*Oryza sativa*) seedlings. *Rice* 12:28

[10] Yu HY, Xu Y, Wang Q, Hu M, Zhang X, et al. 2024. Controlling factors of iron plaque formation and its adsorption of cadmium and arsenic throughout the entire life cycle of rice plants. *Science of the Total Environment* 953:176106

[11] Chu Q, Sha Z, Li D, Feng Y, Xue L, et al. 2023. Oxygen nanobubble-loaded biochars mitigate copper transfer from copper-contaminated soil to rice and improve rice growth. *ACS Sustainable Chemistry & Engineering* 11:5032−5044

[12] Yasin MU, Muhammad S, Chen N, Hannan F, Afzal M, et al. 2025. Nano-engineered biochar enhances soil microbial interactions and maize transcriptomic pathways for cadmium detoxification. *Journal of Hazardous Materials* 495:139029

[13] Li D, Cui H, Cheng Y, Xue L, Wang B, et al. 2021. Chemical aging of hydrochar improves the Cd^{2+} adsorption capacity from aqueous solution. *Environmental Pollution* 287:117562

[14] Shi W, Pan G, Chen Q, Song L, Zhu L, et al. 2018. Hypoxia remediation and methane emission manipulation using surface oxygen nanobubbles. *Environmental Science & Technology* 52:8712−8717

[15] Chen Y, Yang W, Liu H, Mao W, Zhang J, et al. 2025. Phosphorus-loaded magnetic biochar for remediation of cadmium contaminated paddy soil: efficacy and identification of limiting factors. *Journal of Hazardous Materials* 492:138162

[16] Chen Y, Yang W, Liu H, Jing H, Zhang J, et al. 2025. Remediation of cadmium-contaminated paddy soils by phosphorite magnetic biochar: a new insight into soil microbial responses. *Land Degradation & Development* 36:3313−3327

[17] Marcelino KR, Ling L, Wongkiew S, Nhan HT, Surendra KC, et al. 2023. Nanobubble technology applications in environmental and agricultural systems: opportunities and challenges. *Critical Reviews in Environmental Science and Technology* 53:1378−1403

[18] Lan Y, Chu Q, Liu X, Xu S, Li D, t al. 2025. Oxygen-nanobubble-loaded biochar increases soil carbon sequestration in rice paddies. *Soil & Environmental Health* 3:100174

[19] Wu C, Ye Z, Li H, Wu S, Deng D, et al. 2012. Do radial oxygen loss and external aeration affect iron plaque formation and arsenic accumulation and speciation in rice? *Journal of Experimental Botany* 63:2961−2970

[20] Mejia J, Roden EE, Ginder-Vogel M. 2016. Influence of oxygen and nitrate on Fe (hydr)oxide mineral transformation and soil microbial communities during redox cycling. *Environmental Science & Technology* 50:3580−3588

[21] Zhang JY, Zhou H, Gu JF, Huang F, Yang WJ, et al. 2020. Effects of nano-Fe_3O_4-modified biochar on iron plaque formation and Cd accumulation in rice (*Oryza sativa* L.). *Environmental Pollution* 260:113970
[22] Khan ZH, Yu H, Li H, Hassan Kazmi SSU, Han R, et al. 2025. Fe-modified biochar-driven ROS generation in the rhizosphere and their role in microplastic transformation. *Journal of Hazardous Materials* 497:139718
[23] Fresno T, Peñalosa JM, Santner J, Puschenreiter M, Prohaska T, et al. 2016. Iron plaque formed under aerobic conditions efficiently immobilizes arsenic in *Lupinus albus* L roots. *Environmental Pollution* 216:215−222
[24] Yin Y, Wang Y, Ding C, Zhou Z, Tang X, et al. 2024. Impact of iron and sulfur cycling on the bioavailability of cadmium and arsenic in co-contaminated paddy soil. *Journal of Hazardous Materials* 465:133408
[25] Zhang L, Li Y, Wang Y, Liu Z, Kronzucker HJ, et al. 2025. Ion toxicity in waterlogged soils: mechanisms of root response and adaptive strategies. *Frontiers in Plant Science* 16:1653008
[26] Maisch M, Lueder U, Kappler A, Schmidt C. 2019. Iron lung: how rice roots induce iron redox changes in the rhizosphere and create niches for microaerophilic Fe(II)-oxidizing bacteria. *Environmental Science & Technology Letters* 6:600−605
[27] Wang X, Tan X, Dang CC, Liu LY, Wang XW, et al. 2025. Manganese-mediated dissimilatory nitrate reduction to ammonium of nitrate-dependent anaerobic methane oxidation. *Chemical Engineering Journal* 506:159901
[28] Sha Z, Chen Z, Feng Y, Xue L, Yang L, et al. 2020. Minerals loaded with oxygen nanobubbles mitigate arsenic translocation from paddy soils to rice. *Journal of Hazardous Materials* 398:122818
[29] Roberts CS, Ni F, Mitra B. 2021. The zinc and iron binuclear transport center of ZupT, a ZIP transporter from *Escherichia coli*. *Biochemistry* 60:3738−3752
[30] Schulz V, Schmidt-Vogler C, Strohmeyer P, Weber S, Kleemann D, et al. 2021. Behind the shield of Czc: ZntR controls expression of the gene for the zinc-exporting P-type ATPase ZntA in *Cupriavidus metalliduran*s. *Journal of Bacteriology* 203:e00052-21
[31] Liu Y, Chen Y, Chen J, Zhang J, Teng HH. 2024. Combined toxicity of Cd and aniline to soil bacteria varying with exposure sequence. *Environment International* 190:108916
[32] Tang Y, Zhang M, Zhang J, Lyu T, Cooper M, et al. 2021. Reducing arsenic toxicity using the interfacial oxygen nanobubble technology for sediment remediation. *Water Research* 205:117657
[33] He Z, Gao J, Chen X, Ru Y, Zhang D, et al. 2025. Efficient recovery of heavy metals and selenium from wastewater using granular sludge: the crucial role of glutathione (GSH). *Water Research* 270:122826
[34] Zhao X, Dai J, Teng Z, Yuan J, Wang G, et al. 2022. Immobilization of cadmium in river sediment using phosphate solubilizing bacteria coupled with biochar-supported nano-hydroxyapatite. *Journal of Cleaner Production* 348:131221
[35] Song WE, Chen SB, Liu JF, Chen L, Song NN, et al. 2015. Variation of Cd concentration in various rice cultivars and derivation of cadmium toxicity thresholds for paddy soil by species-sensitivity distribution. *Journal of Integrative Agriculture* 14:1845−1854
[36] Zhao FJ, Ma Y, Zhu YG, Tang Z, McGrath SP. 2015. Soil contamination in China: current status and mitigation strategies. *Environmental Science & Technology* 49:750−759